frontiers | Frontiers in Geochemistry

TYPE Original Research
PUBLISHED 10 June 2024
DOI 10.3389/fgeoc.2024.1392021

OPEN ACCESS

EDITED BY
Michael Ojovan,
Imperial College London, United Kingdom

REVIEWED BY
Juan M Menéndez-Aguado,
University of Oviedo, Spain
Nuno Durães,
University of Aveiro, Portugal

*CORRESPONDENCE
A. Surrette,
a.surrette@queensu.ca

RECEIVED 26 February 2024
ACCEPTED 16 April 2024
PUBLISHED 10 June 2024

CITATION
Surrette A, Dobosz A, Lambiv Dzemua G, Falck H and Jamieson HE (2024), Geochemical and mineralogical heterogeneity of the Cantung mine tailings: implications for remediation and reprocessing.
Front. Geochem. 2:1392021.
doi: 10.3389/fgeoc.2024.1392021

Geochemical and mineralogical heterogeneity of the Cantung mine tailings: implications for remediation and reprocessing

A. Surrette[1]*, A. Dobosz[1], G. Lambiv Dzemua[2], H. Falck[2] and H. E. Jamieson[1]

[1]Department of Geological Sciences and Geological Engineering, Queen's University, Kingston, ON, Canada, [2]Northwest Territories Geological Survey, Yellowknife, NWT, Canada

Reprocessing tailings to recover minerals of economic interest and environmental concern can add value to a project and decrease environmental risk, but dealing with heterogeneity within tailings facilities is a challenge. This study investigates the heterogeneity of the Cantung Mine tailings to assess the potential for reprocessing for both value recovery and remediation purposes. The Cantung Mine, Northwest Territories, was a world-class tungsten (W) deposit that was mined periodically from 1962 to 2015. Geochemical analysis of 196 tailings samples shows substantial heterogeneity in the elements of value (tungsten and copper (Cu)) and elements of environmental concern for acid rock drainage (iron (Fe) and sulfur (S)). Tungsten and copper concentrations range from 0.06 to 1.06 wt% W (average 0.32 wt% W) and 0.05 to 0.48 wt% Cu (average 0.23 wt% Cu). Iron and sulfur concentrations range from 8.25 to 34.08 wt% Fe (average 17.14 wt% Fe) and 2.20 to 19.70 wt% S (average 6.7 wt% S). Characterization of 29 samples by scanning electron microscope with automated mineralogy software shows that geochemical heterogeneity corresponds to mineralogical heterogeneity with variability in the concentrations of scheelite ($CaWO_4$), chalcopyrite ($CuFeS_2$) and pyrrhotite ($Fe_{(1-x)}S$). Liberation analyses indicate that additional grinding would be necessary to recover scheelite, chalcopyrite or pyrrhotite. Pyrrhotite with monoclinic and hexagonal-orthorhombic forms were identified. Overall, the Cantung tailings display considerable heterogeneity, which could lead to difficulties in reprocessing for economic or environmental benefit, but characterizing the heterogeneity allows for systems to be optimized.

KEYWORDS

heterogeneity, tailings reprocessing, automated mineralogy, tungsten, scheelite, Cantung Mine, acid rock drainage

1 Introduction

Reprocessing tailings has the potential to add value to a project and mitigate environmental liabilities. As the demand for many commodities increases and geopolitical conflicts cause supply risks, reprocessing mine tailings has been proposed as a solution to recover valuable commodities, but few projects have been successfully implemented (Zinck et al., 2019; Machiels et al., 2021; Maest, 2023). In Canada, the 1911 Gold True North Tailings Operations seems to be the only recently active tailings

reprocessing project based on the authors' research (1911 Gold, 2020). Mine tailings can be heterogeneous due to differences in ore and host rocks, processing methods, depositional history and chemical reactions that may or may not take place, which can make characterization and reprocessing difficult (Jamieson et al., 2015; Nikonow et al., 2019; Mulenshi et al., 2021; Blannin et al., 2022). Reprocessing tailings that have environmental liabilities to extract critical raw materials and reconfigure the storage of the remaining tailings to a more geotechnically and geochemically stable facility could be advantageous for legacy sites, but uncertainty leads to risks (Hudson-Edwards et al., 2011; Mulenshi et al., 2021). The Cantung Mine, a former tungsten mine, provides a case study to assess heterogeneity within a tailings pond and the impacts heterogeneity can have on reprocessing and environmental outcomes.

Heterogeneity within tailings ponds has been documented and studies have shown that heterogeneity can affect vegetation growth for remediation, microbial activity, geotechnical performance, and resource estimation for reprocessing (Liu et al., 2014; Kuhn et al., 2016; Constantinescu et al., 2019; Nikonow et al., 2019; Badiozamani and Beier, 2022). Resource estimation of tailings for reprocessing is currently a barrier to operations due to heterogeneity and a lack of best practices for characterization and economic analyses (Maest, 2023). Heterogeneity also affects the long-term environmental performance of tailings, with the design of the storage facility playing a large role in the outcomes of these effects. A few of the variables that vary within tailings facilities include geochemistry, mineralogy, mineral liberation, grain size, and water content. These variables can also affect the acid rock drainage (ARD) potential of tailings, which is the dominant environmental concern for modern mining operations (URS et al., 2000; Blowes et al., 2014; Dold, 2014). The tailings management strategy implemented at a site must consider these variables, but the strategy implemented can in turn impact variables such as mineralogy and mineral liberation in the long-term as well. Surface tailings disposal strategies can be classified based on water content; conventional slurry tailings have the highest water content at greater than 50% and filtered tailings have the lowest water content, typically ranging from 12% to 20% (Klohn Crippen Berger, 2017; Crystal et al., 2018; Ulrich, 2019; Cacciuttolo Vargas and Pérez Campomanes, 2022). The tailings management strategy chosen is based on initial characterization, but many of the variables can change over time, due to processes such as sulfide oxidation or secondary mineral precipitation. Such changes can make reprocessing challenging (Bussière, 2007; Edraki et al., 2014; Adiansyah et al., 2015; Kinnunen and Kaksonen, 2019; Sarker et al., 2022). Heterogeneity can also make sampling difficult as representative samples are needed to accurately characterize the material (Dinis et al., 2020). The degree of heterogeneity and assessment of what constitutes a representative sample can only be determined through sampling and analysis (Blannin et al., 2022). Automated mineralogy is a tool that can be used to comprehensively analyse multiple samples, providing abundant mineralogical data for characterization (Jamieson et al., 2015). Modal mineralogy, deportment, and mineral liberation are a few of the variables that can be quantified and compared across multiple samples using automated mineralogy software to assess the extent of heterogeneity in a tailings facility, the reprocessing potential, and the environmental risks.

At the Cantung Mine, heterogeneity is expected at multiple scales, from the macro scale of a mine site to the micro scale of mineral structure. Pyrrhotite is the dominant acid-generating mineral and both monoclinic and hexagonal-orthorhombic types have been identified in the tailings (Belzile et al., 2004; MESH Environmental Inc, 2008). The form of pyrrhotite substantially impacts mineral processing, and there is debate about the impact of pyrrhotite structure on the rate of oxidation for environmental considerations (Janzen et al., 2000; Belzile et al., 2004; Multani and Waters, 2018; Tang and Chen, 2022). In this paper, geochemistry, mineralogy, mineral liberation and mineral structure were investigated for Cantung Mine tailings relating to the context of reprocessing potential and sulfide oxidation for tailings management using geochemical and automated mineralogy methods.

2 Site description

The Cantung Mine is a former tungsten mine located in the Mackenzie Mountains in the western region of the Northwest Territories, Canada (Figure 1). The site is within the traditional territory of the Dehcho First Nation and the asserted territory of the Kaska Dene First Nation (North American Tungsten Corporation LTD, 2020). The Nahanni National Park, a UNESCO Heritage Park, is approximately 15 km from the Cantung Mine. The Flat River, which drains into the Nahanni River within the National Park, is adjacent to the Cantung Mine site. Cantung is remotely situated with the nearest community approximately 300 km downstream. The Cantung deposit was discovered in 1959 and operated intermittently from 1962 through 2015. Recovery of tungsten, now considered a critical element, was the primary focus, but copper was also recovered on a limited basis as a second commodity (Fitzpatrick and Bakker, 2011; Hayes and McCullough, 2018; Natural Resources Canada, 2022). Initially, tailings were deposited directly onto the floodplain of the Flat River. In 1965, the first tailings pond (TP1) was constructed, and there are currently five tailings facilities on the site. Tailings Pond 3 (TP3) is the largest tailings facility, storing approximately 1,316,000 m^3 of tailings in a conventional impoundment with the dam crest approximately 35 m above the ground (Tetra Tech, 2022). Recent global tailings dam failures, such as the Mount Polley failure, have increased the demand for safer tailings management, which could include different approaches to tailings storage and handling (Edraki et al., 2014; Lyu et al., 2019). The most recent dam safety review recommended all of the tailings facilities at the Cantung Mine be classified with a *high* dam consequence classification based on environmental and cultural risks, indicating the potential for significant loss or deterioration of habitats and disruption of regional heritage or cultural assets should failure occur (SRK Consulting Inc, 2023). The dam consequence classification is not a measure of risk but is used to determine minimum design standards for tailings facilities (Canadian Dam Association, 2013). Reprocessing and remediating these tailings could be methods to decrease risk or potential impacts. The site is currently in care and maintenance and is owned by the Federal Government after the previous owner, North American Tungsten Corporation Limited (NATCL), defaulted in 2015.

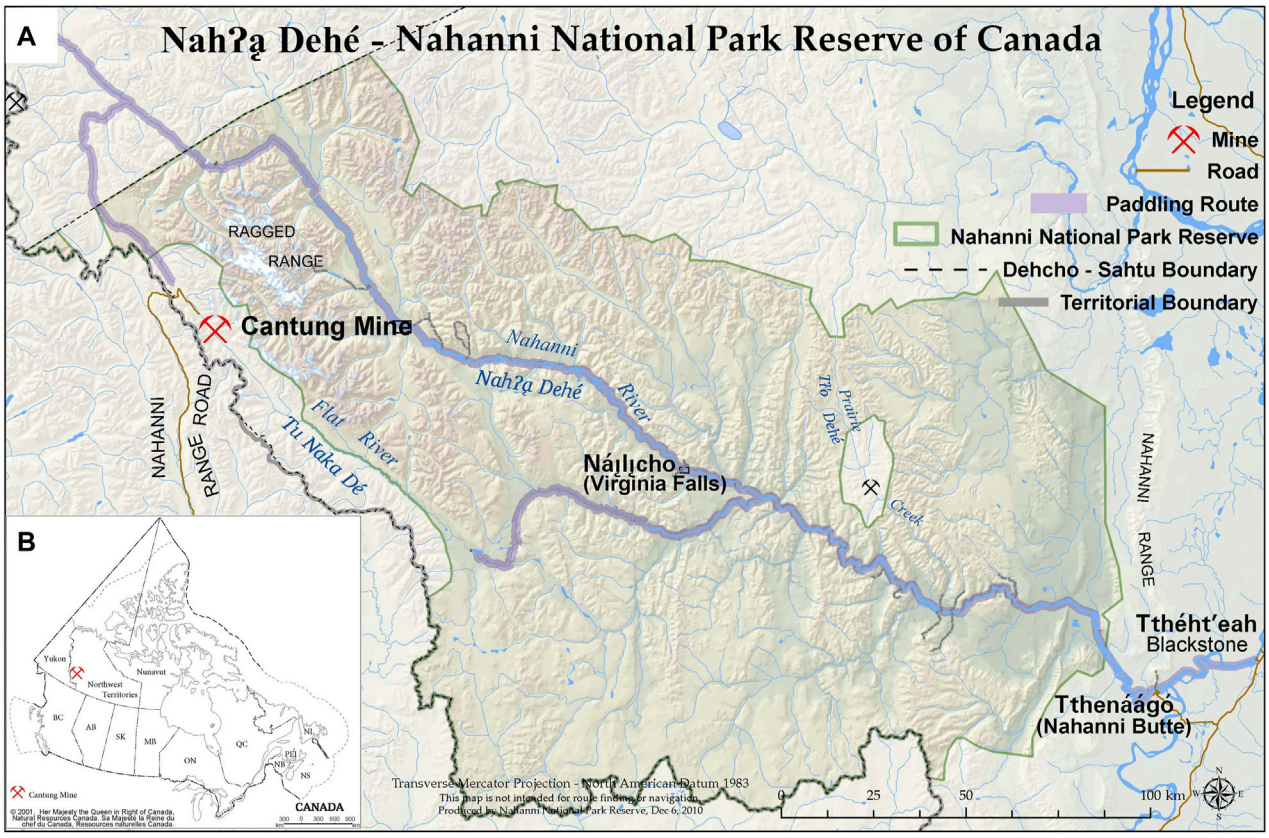

FIGURE 1
Location map for the Cantung Mine. **(A)** Map of the Nahanni National Park Reserve showing the Cantung Mine as the red mine symbol, modified from Nahanni National Park Reserve (2010). **(B)** Map of Canada showing the Cantung Mine Site location, modified from Natural Resources Canada (2001).

The deposit was a tungsten skarn that was formed during and immediately after the Columbian Orogeny. It is associated with felsic intrusions of the Tungsten plutonic suite which were emplaced during the Cretaceous period (Rasmussen et al., 2011). The deposit is composed mainly of carbonate and pelitic rocks, with two primary ore zones, the open pit orebody and the E-zone orebody. The open pit ore zone is hosted by two limestone units, termed the Ore limestone and the Swiss Cheese limestone (Rasmussen et al., 2011). The primary ore mineral was scheelite ($CaWO_4$), and chalcopyrite ($CuFeS_2$) was recovered periodically throughout production (Delaney and Bakker, 2014). While there are abundant carbonate minerals from the limestone host rocks, pyrrhotite ($Fe_{1-x}S$) is also present and is associated with scheelite (Dick and Hodgson, 1982; Rasmussen et al., 2011). The Cantung tailings have previously been classified as potentially acid-generating due to the abundance of pyrrhotite in the tailings (MESH Environmental Inc, 2008; Jamieson et al., 2019).

3 Materials and methods

The methods used in this study include bulk geochemistry, quantitative mineralogy by scanning electron microscope (SEM) equipped with an automated mineralogy suite (Mineral Liberation Analysis; MLA), synchrotron-based micro X-ray diffraction and X-ray fluorescence (μXRD-XRF), and crystallography of pyrrhotite by X-ray diffraction (XRD) and electron microprobe (EMP) analyses. Samples used for these tests include tailings taken from the site and shipped to either CanmetMining, a division of Natural Resources Canada, or Queen's University in 2019, 2020, 2021, and 2022. Data from previous sampling campaigns in 2012 and 2018 were also included. The analyses were focused on samples from TP3 as it is the largest tailings facility on site.

3.1 Sample descriptions

In 2012, multiple core samples were collected by NATCL from TP3 for geochemical analysis to evaluate rare earth element potential. Subsamples of core were collected at depths ranging from 0 to 30 m for analysis by ACME Laboratories, now Bureau Veritas Minerals, and the data has been used in this study. Additional subsamples of the core were collected in 2017 and analysed by SEM-MLA by Jamieson and Dobosz (2019). In 2018, an approximately 60 kg bulk sample was collected from TP3 and analysed for its geochemical composition by CanmetMINING. A grab sample was collected in 2018 from TP3 by Kazamel (2020) and was analysed by SEM-MLA. The 2018 geochemical and mineralogical data has also been included in this study. The 2019 sample was a two-tonne bulk sample from TP3 taken in

TABLE 1 Sample details for materials used in this project.

Sample ID	Year collected	Sample type	Geochemical analysis	Mineralogical analysis
CT-12	2012	Core samples	NATCL at ACME/Bureau Veritas	Jamieson and Dobosz (2019)–Queen's
CT-18	2018	Bulk–60 kg 2 Grab Samples	CanmetMINING	Sample preparation and initial mineralogy: Kazamel (2020)–Queen's
CT-19	2019	Bulk–2000 kg	CanmetMINING Surrette - ALS	Surrette–Queen's
CT-20	2020	Bulk–120 kg	Surrette - ALS	Surrette–Queen's
CT-21	2021	Bulk–200 kg	Surrette - ALS	Surrette–Queen's
CT-22	2022	Bulk–5000 kg	CanmetMINING	Surrette–Queen's

2019 and shipped to CanmetMINING, Ottawa. The sample was then air-dried, homogenized, and split, and two 30 kg pails were shipped to Queen's. Geochemical analysis of the 2019 sample includes data from CanmetMINING analyses and data from Queen's analyses by ALS Geochemistry on different subsamples from the larger bulk sample. The 2020 and 2021 samples were smaller bulk samples from TP3, 120 kg, and 200 kg, respectively. These samples were shipped directly to Queen's in sealed rock pails in August 2020 and August 2021. Both samples went through the same preparation process of initial subsampling of each rock pail for mineralogical and geochemical analysis, followed by air drying for 24 h, homogenization, and splitting, using a rotary sample splitter. The samples were then recombined into pails to obtain homogeneous samples for physical characterization and sulfide oxidation testing. In 2022, an approximately five-tonne bulk sample was taken from TP3 and shipped to CanmetMINING, Ottawa. Data from this sample includes geochemistry, which was analysed by CanmetMINING, and mineralogy, which was analysed at Queen's. All bulk samples were collected at depths ranging from 0 to 5 m. Details for each sample are described in Table 1.

3.2 Bulk geochemistry

One hundred and fifty-two 2012 samples were analysed for whole-rock major and trace element content by inductively coupled plasma emission spectrometry (ICP-ES) after four-acid digestion and by inductively coupled plasma mass spectrometry (ICP-MS) after lithium borate fusion. Quality assurance and quality control (QAQC) measures included analysis of 24 duplicates, 7 standard reference materials (CDN-ME-14, CDN-ME-9), and 28 blanks in addition to the 152 samples. For the elements of interest (tungsten, copper, iron and sulfur) 94% of duplicates were within less than 5% of each other. All blanks measured less than 0.001% tungsten and copper, less than 0.02% iron and less than 0.05% sulfur. Measured values for the standard reference materials were within ±2 standard deviations of the recommended values. Seven samples from 2018, nine from 2019, and eight from 2022 were analysed by CanmetMINING using inductively coupled plasma atomic emission spectroscopy (ICP-AES) following four-acid digestion or lithium metaborate fusion for major or trace elements and ELTRA 2000 for sulfur and carbon. Certified reference materials (MP-2a, RTS-1) and duplicates were measured at regular intervals for the 2018 analyses. Duplicates for the elements of interest were within less than 6% of each other. The MP-2a certified reference material was within ±2 standard deviations of the recommended values for copper and iron but was more than 3 standard deviations less than the recommended value for tungsten. The RTS-3 certified reference material was within ±2 standard deviations of the recommended values for sulfur. Six samples from 2019, eight from 2020, and six from 2021 were analysed at ALS Geochemistry for their major element composition by ICP-AES following lithium borate fusion, trace elements by ICP-MS following four-acid digestion or lithium borate fusion, and total sulfur by induction furnace. The tungsten content of the 2019 and 2020 samples was also analyzed by X-ray fluorescence (XRF) for comparison. Certified reference materials (CDN-W-4, OREAS-101b, OREAS 920, OREAS-45h), duplicates and blanks were analysed to ensure the accuracy and reproducibility of the results. Quality control results for the 2019 and 2020 samples showed that duplicates for tungsten, copper and iron were within less than 2% of each other. Blanks were less than 1 ppm tungsten for fusion and four acid digestions, and less than 0.01% tungsten for XRF analyses. Blanks were less than 0.05% copper and 0.002% iron. For the elements of interest, 91% of the analyses on the certified reference materials were within ±2 standard deviations of the recommended values. The results presented in this work focus on the data from lithium borate fusion analyses for tungsten, four-acid digestion analyses for copper and iron, and either four-acid digestion or induction furnace analyses for sulfur. Induction furnace was used to measure sulfur for all 2018–2022 samples and four-acid followed by ICP-ES was used to measure sulfur for all 2012 samples. No systematic differences in the results were identified.

3.3 Mineralogy

Modal mineralogy, mineral liberation, mineral associations and element deportment were analysed using a scanning electron microscope equipped with an automated mineralogy suite. Subsamples from the 2019, 2020, 2021, and 2022 bulk samples were selected and prepared into polished thin sections and epoxy grain mounts. The 2022 samples were classified using standard sieves into +300 µm, −300 to +150 µm, −150 to +75 µm, −75 to +38 µm, and −38 µm size fractions. One epoxy grain mount prepared by Kazamel (2020) from a sample taken in 2018 and

nine epoxy grain mounts from subsamples of the 2012 core samples were also analysed. Analyses were conducted by the author using the Thermo Scientific™ (formerly FEI) Quanta™ 650 Field Emission Gun (FEG) environmental (E)SEM at Queen's University. The automated mineralogy software used was Mineral Liberation Analysis (MLA). The modes used for analysis included X-ray modal analysis (XMOD) for modal mineralogy and element deportment analysis and sparse phase liberation analysis (SPL-LT) for mineral liberation and association analyses. A mineral reference library was created based on the work done by Kazamel (2020) and manual investigation on the SEM. Automated mineral classification was validated on the SEM by confirming the mineral phase assigned by the program matched the energy dispersive spectroscopy (EDS) spectrum collected manually for a subset of grains. The main sources of error associated with this method included texture and uneven grain surface effects. The percentage of unclassified minerals was reduced to less than 5% by area for all 2018, 2019, 2020, 2021 and 2022 samples by manual validation and library refinement. Agglomeration issues with the 2012 samples resulted in a higher final percentage of unclassified minerals for three samples (CT-12–1, unknowns = 9 area %; CT-12–4, unknowns = 8 area %; CT-12–8, unknowns = 14 area %). The remaining unclassified minerals were a result of fine-grained or complex textures with multiple phases or surfaces that were not flat due to edges or fractures, which caused mixed EDS spectra to be collected.

Synchrotron-based μXRD-XRF was used to identify the mineral forms of iron-oxyhydroxides in the 2020 and 2021 samples. Analyses were conducted at beamline 13-IDE at the Advanced Photon Source (APS), National Argonne Laboratory, Chicago, IL, United States on thin sections that had been analysed by SEM. A monochromatic incident beam at 18 kV with a spot size of 2 μm and a dwell time of 50 ms per pixel was used to collect μXRF and μXRD maps of target grains. Spot μXRD analyses were performed on specific pixels with a measurement time of 10,000 ms per pixel. XRF data was used to investigate the trace chemistry of the target grains and data processing was conducted using Larch software (Version 0.9.46; Newville, 2019). XRD data was processed using Dioptas software (Prescher and Prakapenka, 2015) and HighScore Plus (Version 4.9; (Degen et al., 2014)) for phase identification.

3.4 Pyrrhotite crystallography

To determine the presence of monoclinic and hexagonal pyrrhotite in the Cantung tailings, powder XRD and EMP analyses were performed. Sixteen powder back-mounted samples were analysed by XRD using the Malvern Panalytical Empyrean Powder Diffractometer at Queen's University. A cobalt source was used with a PIXcel3D detector. The data was processed using HighScore Plus (version 4.9) for phase identification and Rietveld refinement. Bulk and separated samples were analysed by XRD, including four bulk samples, four magnetically separated samples, four flotation concentrate samples, and four mineral density separated samples. Magnetic separation was conducted by passing a hand-held sliding magnetic separator over a thin layer of tailings. Flotation concentrate samples were collected from the products of sulfide flotation tests conducted for another study (Collins, 2023). The flotation tests were conducted on samples after magnetic separation. Mineral density separated samples were created using a Jasper table which separated samples based on relative density. The Jasper table was primarily designed to separate zircon grains out of a sample by shaking at a set speed while a slurry ran through grooves in the table. Zircon and pyrrhotite have similar densities (approximately 4.7 and 4.6 g/cm^3, respectively), so tailings samples were passed through the system for 30 min and the material along the ridges that collected dense material was recovered by pipette. The samples were dried under nitrogen gas prior to mounting for XRD.

Forty-eight pyrrhotite grains from samples analysed by SEM-MLA were also analysed by EMP to determine the crystal structure of individual pyrrhotite grains based on iron and sulfur contents. Monoclinic pyrrhotites have greater iron deficiencies, with iron contents of 46.5%–46.8% Fe on a molar basis, and hexagonal to orthorhombic pyrrhotites have lesser iron deficiencies, with iron contents of 47.4%–48.3% Fe on a molar basis (Arnold, 1966; Morimoto et al., 1970; Belzile et al., 2004). Each grain was analysed at two or three different spots for a total of 139 analyses. The JEOL JXA-8230 electron microprobe at QFIR was used in wavelength-dispersive (WDS) mode under operating conditions of 15 kV accelerating potential and 20 nA beam current with a focused beam. Calibration standards included synthetic pyrrhotite, cobaltite, millerite and synthetic digenite. Sulfur (S) Kα was measured on two spectrometers using two different pyrrhotite standards for QAQC purposes. The two diffracting crystals were PET and PETH crystals and the two pyrrhotite standards were S-316 (Fe_7S_8 composition) and S-175 (stoichiometric FeS composition). There were no substantial differences in results across the four test conditions.

4 Results

4.1 Bulk geochemistry

Concentrations of elements of economic interest, tungsten and copper, and elements of environmental concern for sulfide oxidation, iron and sulfur, were assessed and are shown in Figure 2. Tungsten concentrations ranged from 0.06 to 1.06 wt% W, with an average of 0.32 wt% W. The 2019 sample showed the highest concentrations of tungsten, with values ranging from 0.97 to 1.06 wt% W. For all other samples, tungsten concentrations ranged from 0.06 to 0.60 wt% W. Copper concentrations ranged from 0.05 to 0.48 wt% Cu, with an average of 0.23 wt% Cu. Copper concentrations were not elevated in the 2019 sample as the tungsten concentrations were, ranging from 0.13 to 0.15 wt% Cu. The lowest and highest copper concentrations were from the 152 samples analysed from the 2012 sampling year; all other sampling years had minimum and maximum copper concentrations of 0.11 and 0.30 wt% Cu, respectively. Analyses for iron resulted in concentrations ranging from 8.25 to 34.08 wt % Fe with an average of 17.14 wt% Fe. The minimum and maximum values for iron concentrations were also from the 2012 samples, but all other sampling years had minimum values greater than or equal to the average iron concentration of the 2012 samples. The lowest minimum value for a sampling year aside from 2012 at 8.25 wt% Fe

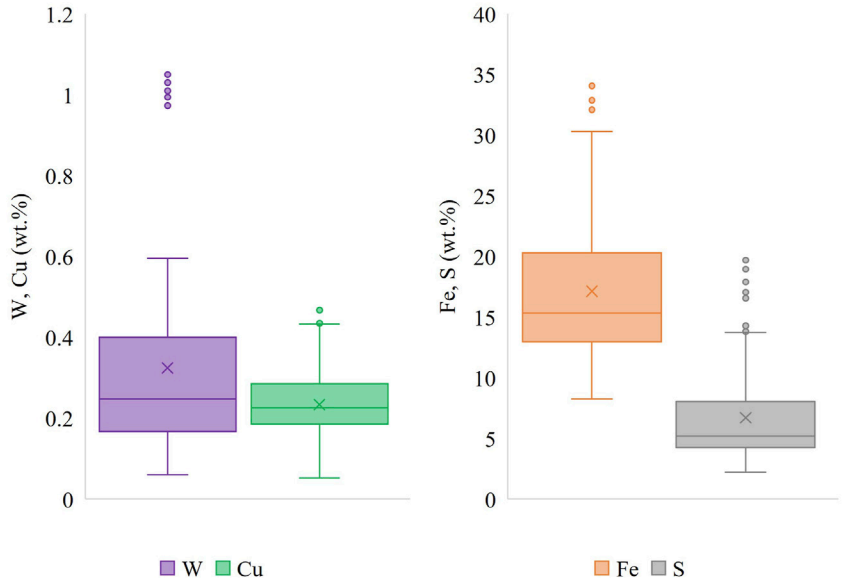

FIGURE 2
Compiled bulk geochemistry results for tungsten (W), copper (Cu), iron (Fe) and sulfur (S) for the Cantung tailings. Data includes samples from all available years, including 2012, 2018, 2019, 2020, 2021 and 2022.

was 15.11 wt% Fe from 2022. The 2019 sample had high iron concentrations ranging from 25.30 to 26.00 wt% Fe, but the 2020 sample had the highest iron concentrations, ranging from 23.20 to 33.10 wt% Fe with an average of 29.10 wt% Fe. Sulfur concentrations ranged from 2.20 to 19.70 wt% S with an average of 6.70 wt% S. Sulfur concentrations were also highest in the 2020 sample, corresponding to iron concentrations, ranging from 13.15 to 19.70 wt% S with an average of 16.96 wt% S.

4.2 Mineralogy

4.2.1 Modal mineralogy

Modal mineralogy was assessed on 19 samples from the 2019, 2020, 2021, and 2022 sampling years, shown in Figure 3, and compared to analyses previously done by Jamieson and Dobosz (2019) and Kazamel (2020) on nine 2012 samples and one 2018 sample, respectively. The main minerals of interest include scheelite ($CaWO_4$) and chalcopyrite ($CuFeS_2$) for economic value and pyrrhotite ($Fe_{1-x}S_x$), iron-oxyhydroxides, sulfates, and carbonates for environmental implications regarding the potential for and evidence of ARD. The elements of economic interest, tungsten and copper, are hosted solely in scheelite and chalcopyrite, respectively, as determined by deportment analyses. Scheelite concentrations ranged from less than 0.1 to 2.1 wt% with an average of 0.5 wt%. The 2019 samples had the highest concentrations of scheelite (1.5–2.1 wt%; average 1.9 wt%), corresponding to the geochemical results for tungsten. Chalcopyrite concentrations ranged from less than 0.1 to 1.4 wt% with an average of 0.6 wt%. The 2021 samples had the highest average concentrations of chalcopyrite (0.4–1.1 wt%; average 0.7 wt%), although a 2012 sample had the sample with the maximum chalcopyrite concentration (sample 1: 1.4 wt%). Pyrrhotite was the main mineral of concern from an environmental viewpoint because of the potential for ARD due to pyrrhotite oxidation. Pyrrhotite concentrations ranged from 0.4 to 31 wt% with an average of 16 wt%. The 2020 sample had the highest pyrrhotite concentrations (24–31 wt%; average 28 wt%), corresponding to the iron and sulfur geochemistry results. Iron-oxyhydroxides can form due to the oxidation of pyrrhotite, and the textures found in these samples included iron-oxyhydroxide rims on pyrrhotite grains and partial or full replacement of pyrrhotite grains. The iron-oxyhydroxides were determined to be primarily goethite (α-FeOOH) or lepidocrocite (γ-FeOOH) based on synchrotron-based μXRD analyses. Iron-oxyhydroxide concentrations ranged from 0.5 to 41 wt% with an average of 18 wt%. The 2019 samples had the highest concentrations of iron-oxyhydroxides (40–41 wt%). Sulfates were another mineral class that potentially formed due to the oxidation of pyrrhotite. The dominant sulfate mineral present in the Cantung tailings was gypsum, although small amounts of jarosite and barite were also present. Sulfate concentrations ranged from 0.1 to 10 wt% with an average of 1.9 wt%. The 2012 samples had the highest concentrations of sulfates (0.4–10 wt%; average 2.7 wt%). Since Cantung was a skarn deposit, carbonate minerals were also present, with concentrations that ranged from 3.1 to 29 wt% with an average of 11 wt%. The primary carbonate mineral was dolomite, followed by calcite and ankerite. The 2018 sample had the highest carbonate mineral concentration at 29 wt%.

4.2.2 Element deportment

Element distributions were analysed to further assess the relationship between geochemistry and mineralogy. Tungsten and copper were hosted solely by scheelite and chalcopyrite, respectively. Pyrrhotite was the dominant host of sulfur for all samples except two, as shown in Figure 4. The 2018 and 2020 samples had the highest distribution of sulfur associated with pyrrhotite, with an average of 94% of sulfur associated with pyrrhotite, compared to averages of 69%, 80%, 81% and 82% of sulfur associated with

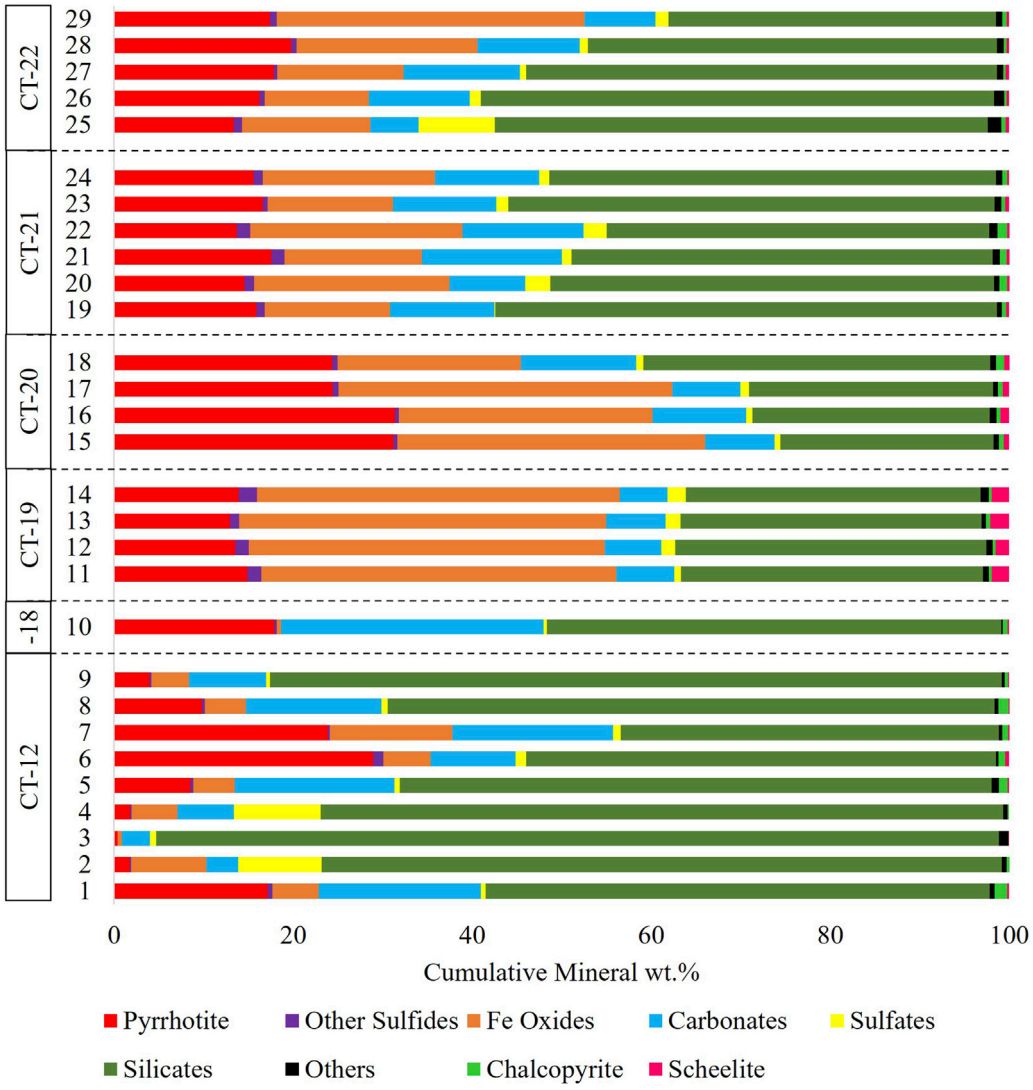

FIGURE 3
Modal mineralogy for the Cantung tailings from sampling years 2012 (from Jamieson and Dobosz, 2019), 2018 (from Kazamel, 2020), and 2019–2022.

pyrrhotite for the 2012, 2019, 2021, and 2022 samples. The two samples that did not show pyrrhotite as the dominant sulfur host (CT-12 samples 2 and 4) had low pyrrhotite concentrations (1.7 and 1.8 wt%) and high gypsum concentrations (9.3 and 9.7 wt%) compared to other samples.

4.2.3 Mineralogical acid-base accounting

With the concentrations of acid-producing and acid-neutralizing minerals known, mineralogically based acid-base accounting was performed. The acid potentials (AP) of chalcopyrite, pyrite, and pyrrhotite were calculated to determine the total AP (Eq. 1, (Paktunc, 1999; Dold, 2017; Karlsson et al., 2018)).

$$AP\ (kg\ CaCO_3\ eq\ t^{-1}) = \sum_{s=1}^{m} X_s * wt.\%\ of\ sulfur\ in\ mineral_s * F_s \quad (1)$$

Where m is the number of iron sulfide minerals that contribute to acid production, X is the concentration of mineral s in the sample (wt%), and F is the calculation factor applied depending on the mineral s. A calculation factor of 31.25 was used to determine the AP of pyrrhotite and pyrite and a factor of 15.62 (31.25/2) was used for the chalcopyrite AP based on the assumption that one mole of calcite neutralizes two moles of acid produced from the oxidation of one mole of sulfur because the system is open and the tailings are exposed to the atmosphere (Eq. 2, (Nicholson et al., 1997)).

$$CaCO_3 + 2H^+ \leftrightarrow Ca^{2+} + CO_2 + H_2O \quad (2)$$

Overall pyrrhotite and pyrite oxidation equations show that the oxidation of one mole of sulfur produces two moles of acid, while the oxidation of one mole of sulfur produces one mole of acid in the overall chalcopyrite oxidation equation (Eqs 3–5), (Dold, 2017)).

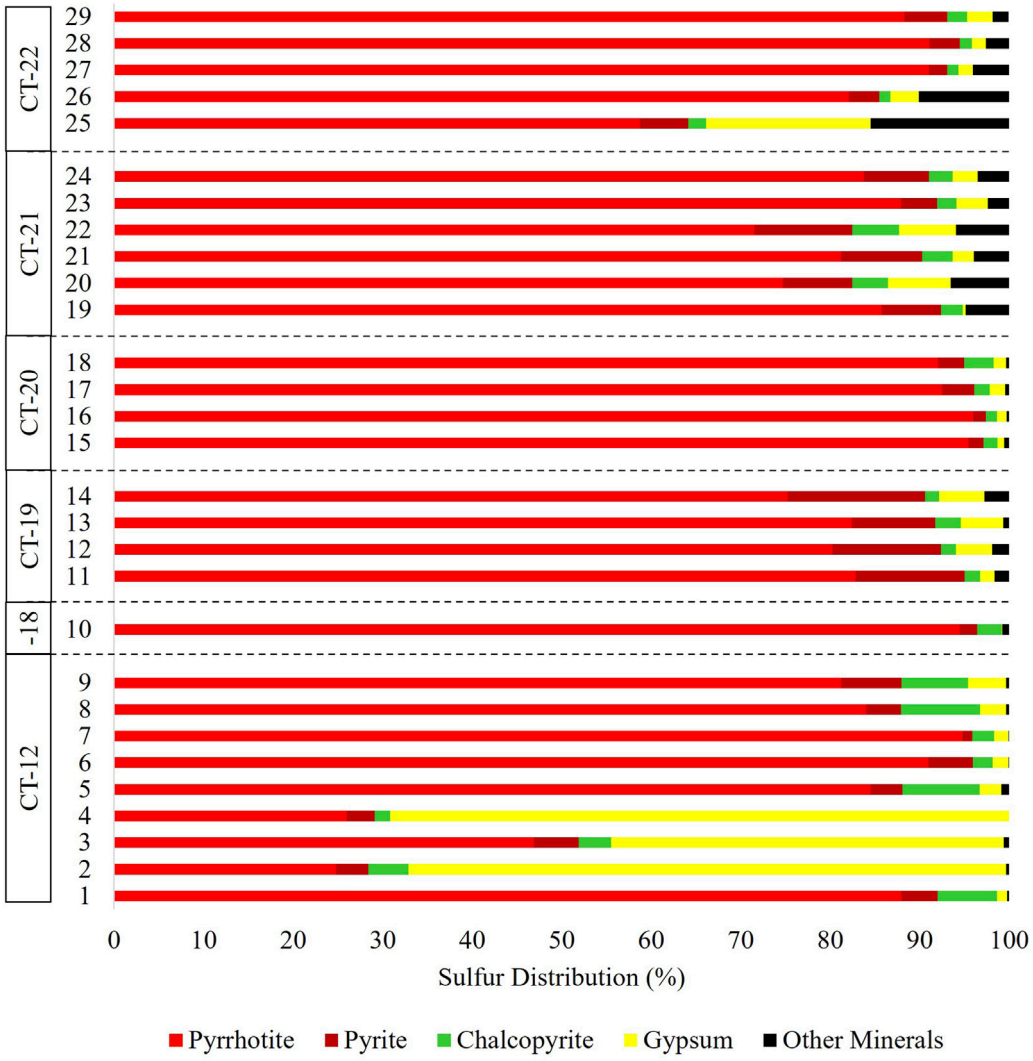

FIGURE 4
MLA-based distribution of sulfur across sulfur-bearing minerals in the Cantung tailings.

$$Fe_{0.9}S + 2.175O_2 + 2.35H_2O \leftrightarrow 0.9Fe(OH)_3 + SO_4^{2-} + 2H^+ \quad (3)$$

$$FeS_2 + 3.75O_2 + 3.5H_2O \leftrightarrow Fe(OH)_3 + 2SO_4^{2-} + 4H^+ \quad (4)$$

$$CuFeS_2 + 4O_2 + 3H_2O \leftrightarrow Cu^{2+} + Fe(OH)_3 + 2SO_4^{2-} + 2H^+ \quad (5)$$

The neutralization potentials (NP) of calcite, dolomite, and ankerite were calculated, including a correction for the iron contribution from ankerite, to determine the total NP (Eq. 6, (Lapakko, 1994; Paktunc, 1999; Frostad et al., 2003; Karlsson et al., 2018)).

$$NP\ (kg\ CaCO_3\ eq\ t^{-1}) = \sum_{i=1}^{k} X_i * (1 - wt.\%\ of\ iron\ in\ mineral_i) * \frac{w_i}{w_{CaCO_3}} * 10 \quad (6)$$

Where k is the number of minerals that contribute to neutralization potential, X is the concentration of mineral i in the sample (wt%), and w is molar mass. The results in Figure 5, below, demonstrate that the 2019, 2020, 2021 and 2022 samples were classified as potentially acid generating (PAG). Two 2012 samples were classified as non-potentially acid generating (NPAG) and five samples from 2012 to 2018 were classified as uncertain based on a neutralization potential ratio of 2. The 2020 samples were determined to have the highest acid potential.

4.2.4 Mineral liberation

Mineral liberation was investigated for scheelite, chalcopyrite and pyrrhotite in the Cantung tailings by SEM-MLA. Liberation of scheelite and chalcopyrite was used to assess recoverability at the current tailings grain size. Figure 6 and Figure 7 show the proportion of scheelite and chalcopyrite, respectively, in liberation classes from 0% to 100% liberation. Liberation of scheelite was heterogenous with values ranging from 5% to 40% of scheelite more than 80% liberated and 11%–92% of scheelite less than 20% liberated (Figure 6). Of the samples analysed, the highest average liberation value for scheelite was approximately 30% of scheelite more than 80% liberated in the 2020, 2021, and middle grain size fractions (from −300 to +38 μm) of the 2022 samples. Scheelite was largely associated with silicates in the 2012, 2018, 2020, 2021 and 2022 samples, and iron oxyhydroxides in the 2019 samples. Liberation of chalcopyrite

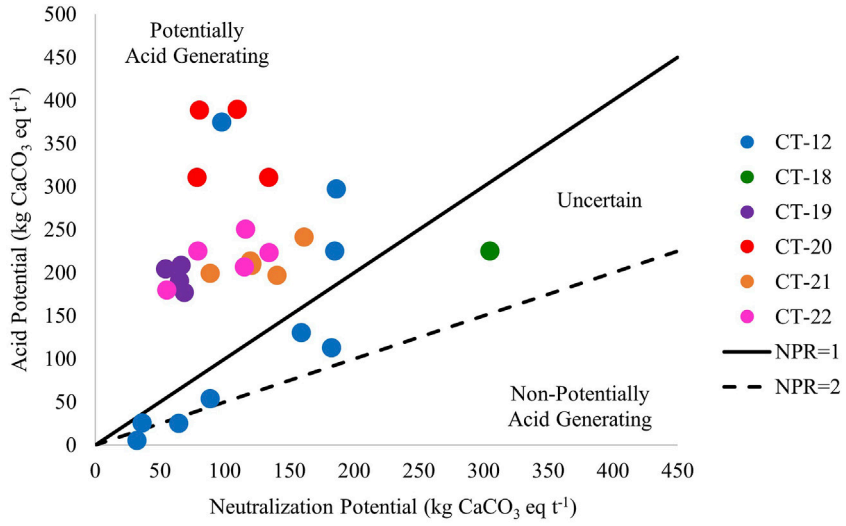

FIGURE 5
Mineralogical acid-base accounting for the Cantung tailings.

showed similar heterogeneity with 1%–60% of chalcopyrite more than 80% liberated and 5%–85% of chalcopyrite less than 20% liberated (Figure 7). The highest average liberation value for chalcopyrite for the samples analysed was approximately 40% of chalcopyrite more than 80% liberated in the 2012 and 2018 samples. Chalcopyrite was most associated with silicates in the 2012, 2018, 2021, and 2022 samples and iron oxyhydroxides in the 2019 and 2020 samples. To assess the availability of pyrrhotite for oxidation or recovery by flotation, the liberation of pyrrhotite was examined. Figure 8 shows the proportion of pyrrhotite in various liberation classes, from 0% to 100% liberation. The distribution of more than 80% liberated pyrrhotite varied from 1% to 70% of pyrrhotite in the sample. The 2012, 2018, 2021 and middle grain size fractions (from −300 to +38 µm) of the 2022 samples had the highest degree of pyrrhotite liberation, with an average of approximately 40% of pyrrhotite more than 80% liberated. The 2019 samples had the lowest degree of pyrrhotite liberation, with an average of 1% of pyrrhotite more than 80% liberated and an average of 95% of pyrrhotite less than 60% liberated. Pyrrhotite grains were most associated with iron oxyhydroxide grains for the 2019, 2020, 2021 and 2022 samples and silicates for the 2012 and 2018 samples. Liberation of scheelite, chalcopyrite and pyrrhotite varied substantially among the 2012 samples, but showed more consistency in other sampling years.

4.3 Pyrrhotite crystallography

The crystal structure of pyrrhotite was analysed to determine the presence of monoclinic, or magnetic pyrrhotite, and hexagonal, or non-magnetic pyrrhotite. Powder XRD was performed on bulk samples and on samples that were separated by hand-magnet, by sulfide flotation and by mineral density. Based on the methods proposed by Arnold (1966) and Graham (1969), monoclinic and hexagonal pyrrhotites were identified in the Cantung tailings. In the range of 51.1°–51.79° 2θ, peaks that are unique to each crystal system were evident. The hexagonal peak for each sample was identified at 2θ values ranging from 51.1° to 51.29° with an average of 51.15°. The monoclinic peaks were present in 75% of samples analysed, with 2θ values ranging from 51.59° to 51.73° with an average of 51.66°. Hexagonal pyrrhotite was dominant in the bulk, flotation concentrate, and density separated samples. Monoclinic pyrrhotite was dominant in the magnetically separated samples. Since monoclinic pyrrhotite is magnetic, the magnetic separate samples were expected to be richer in monoclinic pyrrhotite and the flotation concentrate samples were expected to be richer in hexagonal pyrrhotite, which was left in the sample and recovered by flotation following magnetic separation. The absolute proportions were not quantified, as the samples were complex mixtures of many minerals, which made quantitative Rietveld refinement unreliable when the pyrrhotite was often not the dominant phase in the mixture.

Electron microprobe (EMP) analysis was then used to identify the compositions of pyrrhotite to assess the crystal structure of pyrrhotites showing different degrees of oxidation. XRD analyses determined that both monoclinic and hexagonal pyrrhotite were present in all samples, so pyrrhotite grains at various degrees of oxidation from the 2019, 2020 and 2021 samples were chosen for further investigation. One hundred and thirty-nine spot analyses on 48 pyrrhotite grains from 5 thin sections were analysed by EMPA. Iron content in the pyrrhotites ranged from 46.57% to 49.79% on a molar basis. Only two grains were identified to have an iron deficient, monoclinic (Fe_7S_8) structure, with atomic compositions of 46.7% iron and 53.3% sulfur. All other grains analysed had average atomic compositions of 47.7% iron and 52.3% sulfur, corresponding to a hexagonal or orthorhombic structure that could range from Fe_9S_{10} to $Fe_{11}S_{12}$. The two monoclinic pyrrhotite grains were from a 2019 sample and a 2020 sample, although it is expected that monoclinic and hexagonal pyrrhotite are both present in all samples, with hexagonal being the dominant structure. Both intact and oxidized pyrrhotite grains were analysed, which showed that the degree of oxidation of a pyrrhotite grain was

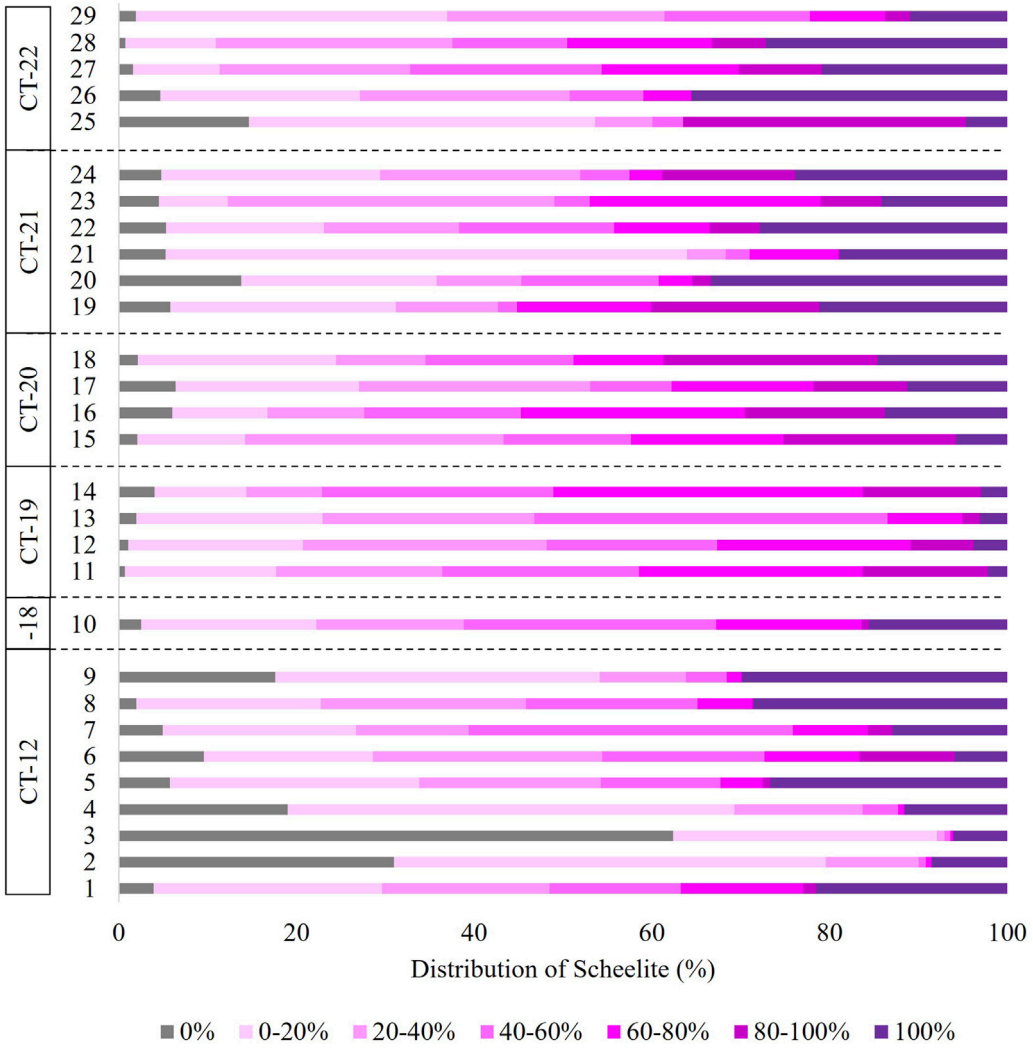

FIGURE 6
Distribution of scheelite across liberation classes ranging from 0% liberated to 100% liberated.

not indicative of its structure for these samples. The two monoclinic grains identified were strongly oxidized, but compositions that align with hexagonal pyrrhotites were determined in both intact and strongly oxidized grains. Target grains with hexagonal and monoclinic structure are shown in Figure 9.

5 Discussion

The Cantung tailings displayed heterogeneity in geochemistry and mineralogy. This heterogeneity could be caused by many factors including heterogeneity of the ore body, changes in the processing circuit, the tailings management strategy, and reactions that took place within the tailings facility. Focusing on reprocessing potential, there is one pocket of the tailings facility where tungsten grades are above the average ore grade of the mine (2019 sample–average 1.01 wt% W, n = 15, compared to an average ore grade of 0.64 wt% W (Delaney and Bakker, 2014)), while the majority of the tailings facility had lower grades, with an average of 0.27 wt% W (2012, 2018, 2020, 2021 and 2022 samples, n = 181). Primary tungsten grades at operating mines generally range from 0.2 to 1.1 wt% W and reported tungsten grades of tailings deposits range from 0.05 to 0.1 wt% W (Han et al., 2021). Comparing the tungsten concentrations of the Cantung tailings to other sites indicates that there is potential for reprocessing, but this is based only on grade, and other operational and economic factors must be evaluated to determine the viability of the project. The tungsten at Cantung is hosted solely in scheelite, so the recovery of tungsten requires the processing of only one mineral, but while the 2019 sample has the highest concentrations of tungsten and scheelite, it has low proportions of fully liberated scheelite. Only 5%–16% of the scheelite in the 2019 sample is more than 80% liberated, with 49%–87% of scheelite less than 60% liberated. The 2020, 2021 and 2022 samples have higher average scheelite liberation values of 29%, 31% and 30% of scheelite more than 80% liberated, respectively, but scheelite concentrations are lower, ranging from 0.3 to 1 wt% scheelite. The 2018 sample has similar scheelite liberation values, with 16% of scheelite more than 80%

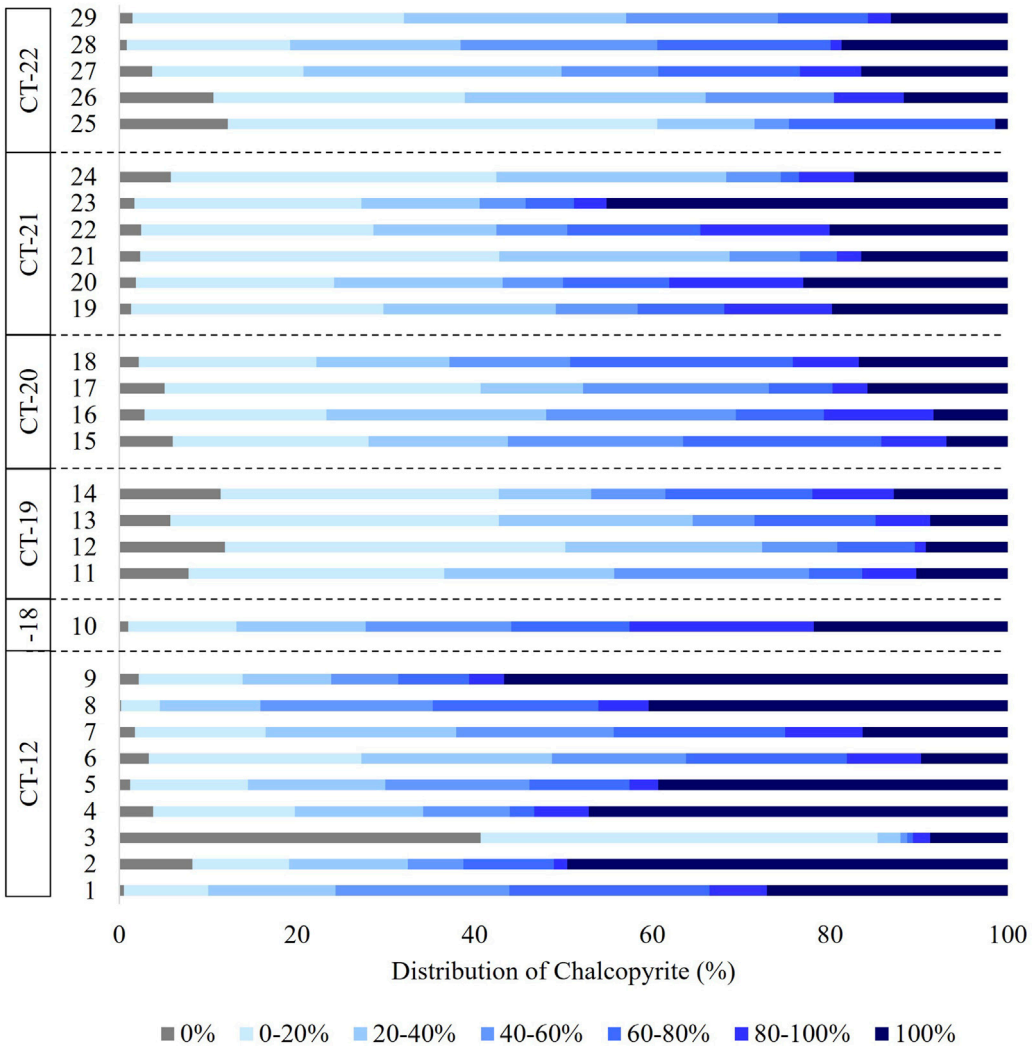

FIGURE 7
Distribution of chalcopyrite across liberation classes ranging from 0% liberated to 100% liberated.

liberated and 67% of scheelite less than 60% liberated, and some 2012 samples have even lower degrees of scheelite liberation, with up to 94% of scheelite less than 60% liberated, and these samples have scheelite concentrations of less than 0.4 wt% scheelite. The 2022 samples were sieved before analysis under SEM-MLA, thus separated by grain size, and this showed that the scheelite concentrations were similar in all size fractions, ranging from 0.3 to 0.4 wt% scheelite. Scheelite liberation was lowest in the +300 μm size fraction, but the fines (−38 μm) fraction had the highest proportion (78%) of scheelite less than 60% liberated.

The reprocessing potential and heterogeneity associated with copper differs from that of tungsten. The average grade of copper in the tailings facilities is 0.23 wt% Cu, while copper grades of operating mines averaged 0.62–0.65 wt% Cu globally in 2015 (Calvo et al., 2016; Alvear Flores et al., 2020). Copper is hosted solely by one mineral, chalcopyrite, and samples with higher concentrations of chalcopyrite have higher degrees of chalcopyrite liberation. The 2021 samples have an average chalcopyrite concentration of 0.7 wt% chalcopyrite with an average of 33% of chalcopyrite more than 80% liberated and 59% less than 60% liberated, compared to the 2019 and 2022 samples, which have average chalcopyrite concentrations of 0.3 wt% chalcopyrite with an average of 16% of chalcopyrite more than 80% liberated and 72% of chalcopyrite less than 60% liberated. While the 2019 sample had the highest concentration of tungsten, it had lower average concentrations of copper compared to other samples. The average copper concentration across all samples was 0.23 wt% Cu, while the average of the 2019 samples was 0.14 wt% Cu. In the samples separated by grain size, the +300 μm and −38 μm size fraction samples had the highest concentrations of chalcopyrite at 0.5 wt%. The intermediate size fractions had concentrations of 0.3 wt% chalcopyrite. Similar to scheelite, chalcopyrite liberation was lowest in the +300 μm size fraction, with 1% of chalcopyrite more than 80% liberated, but the −300 to +150 μm size fraction had the highest proportion (80%) of chalcopyrite less than 60% liberated.

Creating a reprocessing flow sheet that could recover scheelite and chalcopyrite in an economically feasible manner will be challenging due to the heterogeneity within this tailings pond.

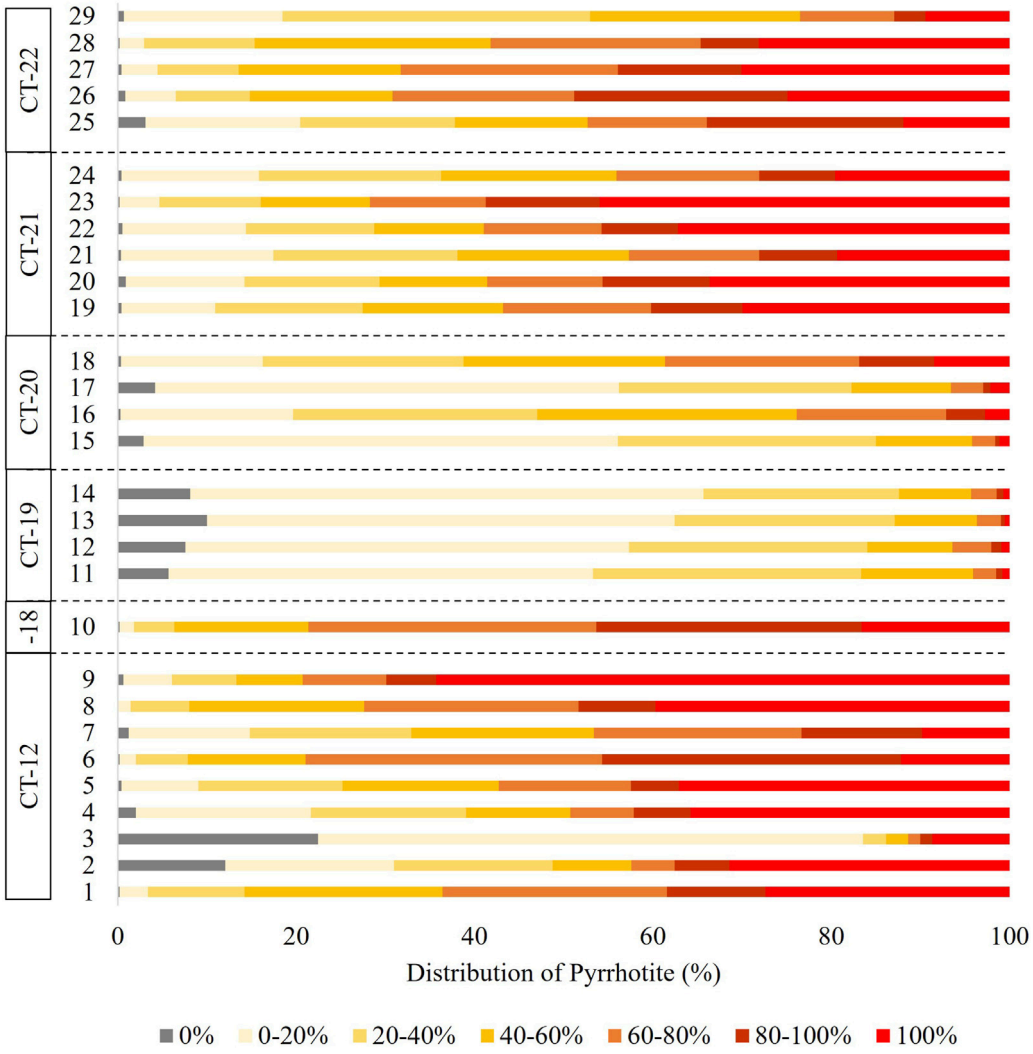

FIGURE 8
Distribution of pyrrhotite across liberation classes ranging from 0% liberated to 100% liberated.

While the highest concentrations of scheelite and chalcopyrite are in the largest grain size fraction analysed, additional grinding would be necessary to improve liberation for recovery due to liberation. There is also no systematic method to interpolate the grade of tungsten and copper in the tailings facility as details about tailings deposition, such as specific periods when copper was not recovered and corresponding spigot points, are not available and there are substantial variations in close proximity. However, characterization of the potential extremes allows for a moderated plan to be developed, which may miss recovery of the outliers, but could capture most of the value.

From an environmental perspective, tailings can be managed at different points throughout the mining cycle; the amount of tailings can be reduced from the beginning depending on the extraction method chosen, the composition of tailings can be altered by removing minerals of interest or adding reagents during processing, and the behaviour of tailings can be affected by the tailings storage method. The strategies chosen at each of these points strongly affects environmental outcomes and the effect of the storage method is demonstrated by the different results seen from the Flat River tailings and the impounded tailings at the Cantung Mine. The Flat River tailings were deposited on the floodplain of the Flat River as a slurry with no manufactured containment in 1962. In 1963, the first tailings facility, tailings pond 1 (TP1), was constructed using the upstream dam method. From 1965 to 2015, tailings were deposited as a slurry into 5 dam style tailings facilities (MESH Environmental Inc, 2008; SRK Consulting (Canada) Inc., 2023). The differences in behaviour of the tailings are remarkable. The Flat River tailings have oxidized and have acidic pore waters, while the impounded tailings show little evidence of oxidation and have near-neutral pore waters (MESH Environmental Inc, 2008; Kazamel et al., 2023). Understanding the differences in behaviour of the Cantung tailings under various storage conditions is crucial for minimizing environmental impacts, and characterization is needed to do this. The main environmental concern for the Cantung tailings is acid rock drainage caused from the oxidation of pyrrhotite. Pyrrhotite is abundant in all samples analysed, and mineralogically based acid-base accounting indicates that most

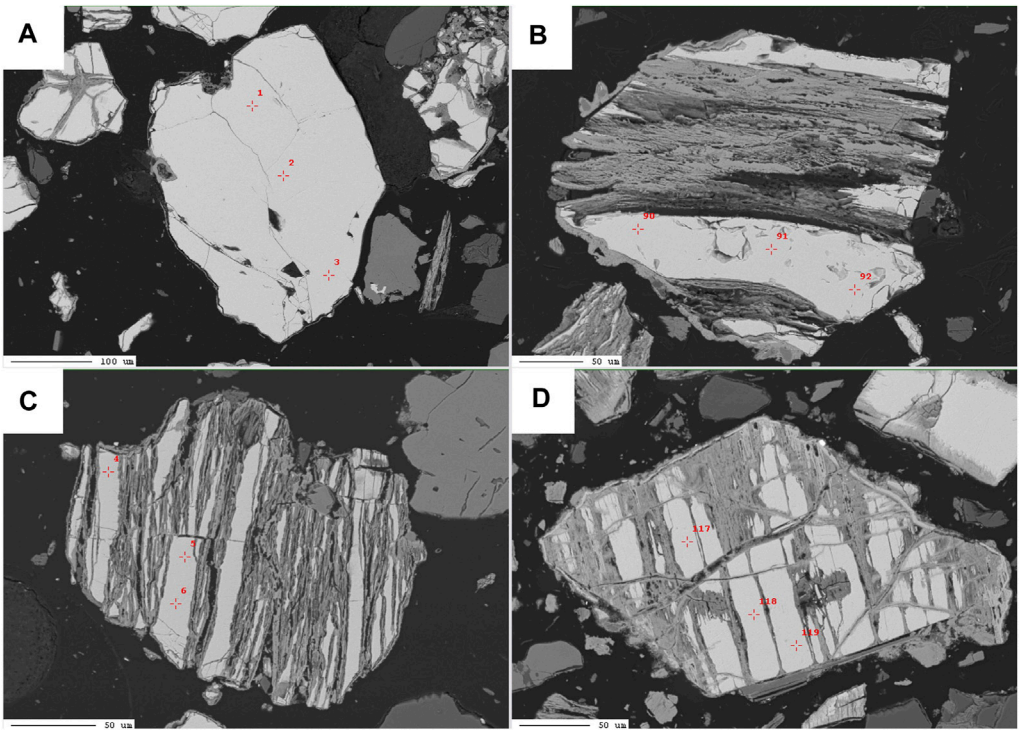

FIGURE 9
Backscatter electron (BSE) images of target pyrrhotites for EMP analyses to determine crystal structure based on iron concentrations. **(A)** An intact pyrrhotite with hexagonal structure ($Fe_{11}S_{12}$). **(B)** An oxidized pyrrhotite with hexagonal structure ($Fe_{11}S_{12}$). **(C)** and **(D)** Oxidized pyrrhotites with monoclinic structure (Fe_7S_8).

samples are classified as potentially acid generating, meaning that if the tailings were stored using an unsaturated method, such as filtered tailings, oxidation would occur and create acid drainage as there are insufficient carbonates to neutralize the acid produced. Environmental desulfurization is a potential solution to this issue, although differences in the condition and structure of pyrrhotite in the tailings should be taken into consideration to optimize recovery by flotation (Becker et al., 2010; Tang and Chen, 2022). Two forms of pyrrhotite are present in the tailings, a monoclinic, magnetic form and a hexagonal-orthorhombic, non-magnetic form. No obvious link between degree of oxidation of the pyrrhotite and its structure was determined throughout this research, although grains of both structures were found. Pyrrhotite liberation also varies considerably throughout the samples analysed. The 2019 and 2020 samples have low pyrrhotite liberation, with averages of 1% and 7% of pyrrhotite more than 80% liberated, respectively, and 95% and 82% of pyrrhotite less than 60% liberated, respectively. The 2018 and 2021 samples have high pyrrhotite liberation, with an average of 42% of pyrrhotite more than 80% liberated and 41% of pyrrhotite less than 60% liberated. Pyrrhotite is dominantly associated with iron oxyhydroxides, indicating that oxidation has occurred, which could make reprocessing difficult as there are fewer fresh surfaces available for the flotation process. This is demonstrated by the 2019 and 2020 samples, and the finest grain size fraction analysed (−38 μm; CT-22–sample 29), which have high concentrations of iron oxyhydroxides and low pyrrhotite liberation. Sulfate precipitation is also evident in some 2012 samples (CT-12, samples 2 and 4). The variability in the mineralogy of the 2012 samples, which were subsampled from core samples taken from various locations throughout TP3, emphasizes the spatial heterogeneity of the tailings facility and the differences that have resulted over time. However, even samples with low pyrrhotite concentrations contain oxidation products (iron oxyhydroxides and gypsum). Since oxidation has occurred to some extent throughout the tailings facility, grinding would be necessary to increase liberation and generate fresh surfaces prior to reprocessing for desulfurization. One of the advantages of reprocessing tailings is that the grinding requirements are reduced because the tailings have already gone through the processing circuit. However, in the case of the Cantung tailings, liberation analysis has shown that additional grinding is likely necessary to increase the potential for recovering scheelite or chalcopyrite for value, or pyrrhotite for environmental management.

6 Conclusion

Characterization of mine tailings is important for assessing heterogeneity, reprocessing potential and remediation strategies. Heterogeneity was confirmed across multiple scales and variables, including bulk geochemistry, modal mineralogy, mineral liberation and mineral structure for the Cantung Mine tailings. Geochemical analyses showed that the Cantung tailings host tungsten and copper concentrations ranging from 0.06 to 1.06 wt% W and 0.05 to 0.48 wt % Cu, respectively, throughout the tailings facility, indicating potential spatial heterogeneity issues for reprocessing. However,

an average grade of approximately 0.30 wt% W and an average grade of 0.23 wt% Cu were reported. Both tungsten and copper are considered critical or strategic minerals by Canada and the EU, and tungsten is also considered a critical mineral by the United States (Hayes and McCullough, 2018; Natural Resources Canada, 2022; U.S. Geological Survey, 2022; European Commission Directorate-General for Internal Market et al., 2023. The tungsten grades are well above other reported tungsten tailings facility grades, making it a potential opportunity for economic recovery. Other challenges around liberation and grain size could be problematic for reprocessing. Modal mineralogy, element deportment, and mineral liberation and associations were assessed using a scanning electron microscope with automated mineralogy software to analyse and compare multiple samples. Scheelite and chalcopyrite were present in all samples and were the sole hosts of tungsten and copper, respectively. Liberation of scheelite and chalcopyrite was heterogeneous and varied by sample and by grain size. The Cantung Mine tailings also have a high risk for acid rock drainage due to the concentrations of pyrrhotite. Variable degrees of oxidation of the pyrrhotites were visible, indicating that oxidation has occurred to some extent in the current impoundments, although the tailings pore waters remain near-neutral. Environmental desulfurization by flotation would require grinding to produce fresh surfaces of pyrrhotite and the tailings management strategy will affect the future behaviour of pyrrhotite in these tailings. Understanding the factors that will impact both reprocessing potential and environmental outcomes for mine tailings and constraining heterogeneity through characterization is imperative for designing impactful tailings management strategies.

Data availability statement

The data presented in the study are available at https://hdl.handle.net/1974/33107.

Author contributions

AS: Conceptualization, Investigation, Methodology, Writing–original draft, Writing–review and editing. AD: Investigation, Writing–review and editing. GL: Resources, Writing–review and editing. HF: Resources, Writing–review and editing. HJ: Conceptualization, Project administration, Supervision, Writing–review and editing.

Funding

The author(s) declare that financial support was received for the research, authorship, and/or publication of this article. This project was supported by the Northwest Territories Geological Survey Contribution Agreement 63040/60123, NSERC Northern Research Award 305500 awarded to HJ, NSERC Discovery Grant 03736 awarded to HJ, and the Ontario Graduate Scholarship awarded to AS.

Acknowledgments

The authors would like to acknowledge North American Tungsten Corporation Limited for their assistance with sample collection, and Dr. M. Leybourne, Queen's University, for his guidance with the bulk geochemistry work. Shannon Shaw, pHase Geochemistry, provided valuable advice during the development of the project, the synchrotron μXRD-XRF analyses could not have been performed without the assistance and guidance of Dr. M. Newville and Dr. A. Lanzirotti at beamline 13-IDE, Advanced Photon Source (APS), Argonne National Laboratory, and the use of the Jasper table for mineral separation was possible thanks to the guidance of Dr. C. Spencer, Queen's University. The authors would also like to thank Dr. R. Peterson, Emeritus Professor, Queen's University, and B. Joy, Queen's Facility for Isotope Research, for assistance with pyrrhotite XRD and EMP analyses, respectively.

Conflict of interest

The authors declare that the research was conducted in the absence of any commercial or financial relationships that could be construed as a potential conflict of interest.

Publisher's note

References

Adiansyah, J. S., Rosano, M., Vink, S., and Keir, G. (2015). A framework for a sustainable approach to mine tailings management: disposal strategies. *J. Clean. Prod.* 108, 1050–1062. doi:10.1016/j.jclepro.2015.07.139

Arnold, R. G. (1966). Mixtures of hexagonal and monoclinic pyrrhotite and the measurement of the metal content of pyrrhotite by X-ray diffraction. *Am. Mineralogist* 51 (7), 1221–1227.

Badiozamani, M. M., and Beier, N. (2022). Estimating the potential differential settlement of a tailings deposit based on consolidation properties heterogeneity. *Appl. Sci.* 12 (12), 6206. doi:10.3390/app12126206

Becker, M., Villiers, J. d., and Bradshaw, D. (2010). The flotation of magnetic and non-magnetic pyrrhotite from selected nickel ore deposits. *Miner. Eng.* 23 (11-13), 1045–1052. doi:10.1016/j.mineng.2010.07.002

Belzile, N., Chen, Y.-W., Cai, M.-F., and Li, Y. (2004). A review on pyrrhotite oxidation. *J. Geochem. Explor.* 84 (2), 65–76. doi:10.1016/j.gexplo.2004.03.003

Blannin, R., Frenzel, M., Tolosana-Delgado, R., and Gutzmer, J. (2022). Towards a sampling protocol for the resource assessment of critical raw materials in tailings storage facilities. *J. Geochem. Explor.* 236, 106974. doi:10.1016/j.gexplo.2022.106974

Blowes, D. W., Ptacek, C. J., Jambor, J. L., Weisener, C. G., Paktunc, D., Gould, W. D., et al. (2014). "The geochemistry of acid mine drainage," in *Treatise on geochemistry*. Editors D. Holland, and K. K. Turekian (USA: ISBN), 131–190.

Bussière, B. (2007). Colloquium 2004: hydrogeotechnical properties of hard rock tailings from metal mines and emerging geoenvironmental disposal approaches. *Can. Geotechnical J.* 44 (9), 1019–1052. doi:10.1139/t07-040

Cacciuttolo Vargas, C., and Pérez Campomanes, G. (2022). Practical experience of filtered tailings technology in Chile and Peru: an environmentally friendly solution. *Minerals* 12 (7), 889. doi:10.3390/min12070889

Calvo, G., Mudd, G., Valero, A., and Valero, A. (2016). Decreasing ore grades in global metallic mining: a theoretical issue or a global reality? *Resources* 5 (4), 36. doi:10.3390/resources5040036

Canadian Dam Association (2013). *Dam safety guidelines 2007*. 2013 Edition.

Collins, A. (2023). *Reprocessing of the Cantung mine tailings*. MASc: Queen's University.

Constantinescu, P., Neagoe, A., Nicoara, A., Grawunder, A., Ion, S., Onete, M., et al. (2019). Implications of spatial heterogeneity of tailing material and time scale of vegetation growth processes for the design of phytostabilisation. *Sci. Total Environ.* 692, 1057–1069. doi:10.1016/j.scitotenv.2019.07.299

Crystal, C., Hore, C., and Ezama, I. (2018). "Filter-pressed dry stacking: design considerations based on practical experience," in *Tailings and mine waste 2018* (Colorado, USA: Keystone).

Degen, T., Sadki, M., Bron, E., König, U., and Nénert, G. (2014). The HighScore suite. *Powder Diffr.* 29 (S2), S13–S18. doi:10.1017/s0885715614000840

Delaney, B., and Bakker, F. J. (2014). *Technical report on the Cantung mine, Northwest Territories, Canada*. Canada: North American Tungsten LTD.

Dick, L. A., and Hodgson, C. J. (1982). The MacTung W-Cu(Zn) contact metasomatic and related deposits of the northeastern Canadian cordillera. *Econ. Geol.* 77 (4), 845–867. doi:10.2113/gsecongeo.77.4.845

Dinis, M. d. L., Fiuza, A., Futuro, A., Leite, A., Martins, D., Figueiredo, J., et al. (2020). Characterization of a mine legacy site: an approach for environmental management and metals recovery. *Environ. Sci. Pollut. Res.* 27 (9), 10103–10114. doi:10.1007/s11356-019-06987-x

Dold, B. (2014). Evolution of acid mine drainage formation in sulphidic mine tailings. *Minerals* 4 (3), 621–641. doi:10.3390/min4030621

Dold, B. (2017). Acid rock drainage prediction: a critical review. *J. Geochem. Explor.* 172, 120–132. doi:10.1016/j.gexplo.2016.09.014

Edraki, M., Baumgartl, T., Manlapig, E., Bradshaw, D., Franks, D. M., and Moran, C. J. (2014). Designing mine tailings for better environmental, social and economic outcomes: a review of alternative approaches. *J. Clean. Prod.* 84, 411–420. doi:10.1016/j.jclepro.2014.04.079

European Commission Directorate-General for Internal MarketGrohol, M., and Veeh, C. (2023). *Study on the critical raw materials for the EU 2023 – final report*. USA: Publications Office of the European Union.

Fitzpatrick, K., and Bakker, F. J. (2011). *Technical report on the Cantung mine, Northwest Territories, Canada*. Canada: North American Tungsten LTD.

Flores, G. A., Risopatron, C., and Pease, J. (2020). Processing of complex materials in the copper industry: challenges and opportunities ahead. *JOM* 72 (10), 3447–3461. doi:10.1007/s11837-020-04255-9

Frostad, S. R., Price, W. A., and Bent, H. (2003). "Operational NP determination - accounting for iron manganese carbonates and developing a site-specific fizz rating," in *Sudbury '95, mining and the environment III* (China: Sudbury, Ontario).

Gold (2020). True North complex - tailings operation. Available at: https://1911gold.com/assets/true-north-complex/(Accessed September 26, 2023).

Graham, A. R. (1969). Quantitative determination of hexagonal and monoclinic pyrrhotites by X-ray diffraction. *Can. Mineralogist* 10 (1), 4–24.

Han, Z., Golev, A., and Edraki, M. (2021). A review of tungsten resources and potential extraction from mine waste. *Minerals* 11 (7), 701. doi:10.3390/min11070701

Hayes, S. M., and McCullough, E. A. (2018). Critical minerals: a review of elemental trends in comprehensive criticality studies. *Resour. Policy* 59, 192–199. doi:10.1016/j.resourpol.2018.06.015

Hudson-Edwards, K. A., Jamieson, H. E., and Lottermoser, B. G. (2011). Mine wastes: past, present, future. *Elements* 7 (6), 375–380. doi:10.2113/gselements.7.6.375

Jamieson, H. E., and Dobosz, A. (2019). *Characterization of the Cantung tailings by mineral liberation analysis 2019: report to NTGS*.

Jamieson, H. E., Kazamel, B., Leybourne, M., Dobosz, A., and Falck, H. (2019). "Increasing value and decreasing environmental risk by reprocessing and stabilizing tungsten tailings at Cantung mine, NT, Canada," in *15th society for geology applied to mineral deposits biennial meeting 2019* (UK: SGA).

Jamieson, H. E., Walker, S. R., and Parsons, M. B. (2015). Mineralogical characterization of mine waste. *Appl. Geochem.* 57, 85–105. doi:10.1016/j.apgeochem.2014.12.014

Janzen, M. P., Nicholson, R. V., and Scharer, J. M. (2000). Pyrrhotite reaction kinetics: reaction rates for oxidation by oxygen, ferric iron, and for nonoxidative dissolution. *Geochimica Cosmochimica Acta* 64 (9), 1511–1522. doi:10.1016/S0016-7037(99)00421-4

Karlsson, T., Raisanen, M. L., Lehtonen, M., and Alakangas, L. (2018). Comparison of static and mineralogical ARD prediction methods in the Nordic environment. *Environ. Monit. Assess.* 190 (12), 719–729. doi:10.1007/s10661-018-7096-2

Kazamel, B. (2020). *Factors controlling tungsten mobility in W-Cu skarn tailings from the Cantung mine Northwest Territories*. Canada. MSc: Queen's University.

Kazamel, B. G., Jamieson, H. E., Leybourne, M. I., and Falck, H. (2023). Factors controlling tungsten mobility in W-Cu skarn tailings. *Chem. Geol.* 630, 121487. doi:10.1016/j.chemgeo.2023.121487

Kinnunen, P. H. M., and Kaksonen, A. H. (2019). Towards circular economy in mining: opportunities and bottlenecks for tailings valorization. *J. Clean. Prod.* 228, 153–160. doi:10.1016/j.jclepro.2019.04.171

Klohn Crippen Berger (2017). Study of tailings management technologies. *Mine Environ. Neutral Drain.* 2.50.1.

Kuhn, K., Meima, J. A., Rammlmair, D., and Ohlendorf, C. (2016). Chemical mapping of mine waste drill cores with laser-induced breakdown spectroscopy (LIBS) and energy dispersive X-ray fluorescence (EDXRF) for mineral resource exploration. *J. Geochem. Explor.* 161, 72–84. doi:10.1016/j.gexplo.2015.11.005

Lapakko, K. A. (1994). Evaluation of neutralization potential determinations for metal mine waste and a proposed alternative. *J. Am. Soc. Min. Reclam.* 1994 (1), 129–137. doi:10.21000/jasmr94010129

Liu, J., Hua, Z. S., Chen, L. X., Kuang, J. L., Li, S. J., Shu, W. S., et al. (2014). Correlating microbial diversity patterns with geochemistry in an extreme and heterogeneous environment of mine tailings. *Appl. Environ. Microbiol.* 80 (12), 3677–3686. doi:10.1128/AEM.00294-14

Lyu, Z., Chai, J., Xu, Z., Qin, Y., and Cao, J. (2019). A comprehensive review on reasons for tailings dam failures based on case history. *Adv. Civ. Eng.* 2019, 1–18. doi:10.1155/2019/4159306

Machiels, L., Frenzel, M., Goldmann, D., Illikainen, M., and Pfister, S. (2021). Preface to the thematic section: mine tailings: problem or opportunity? Towards a combined remediation and resource recovery approach. *J. Sustain. Metallurgy* 7 (4), 1440–1443. doi:10.1007/s40831-021-00468-7

Maest, A. (2023). Remining for renewable energy metals: a review of characterization needs, resource estimates, and potential environmental effects. *Minerals* 13 (11), 1454. doi:10.3390/min13111454

MESH Environmental Inc (2008). *Geochemical characterization of the Cantung mine tailings*. USA: NWT.

Morimoto, N., Nakazawa, H., Nishigucmi, K., and Tokonami, M. (1970). Pyrrhotites: stoichiometric compounds with composition $fe_{n-1}S_n$ (n≥8). *Science* 168, 964–966. doi:10.1126/science.168.3934.964

Mulenshi, J., Gilbricht, S., Chelgani, S. C., and Rosenkranz, J. (2021). Systematic characterization of historical tailings for possible remediation and recovery of critical metals and minerals – the Yxsjöberg case. *J. Geochem. Explor.* 226, 106777. doi:10.1016/j.gexplo.2021.106777

Multani, R. S., and Waters, K. E. (2018). A review of the physicochemical properties and flotation of pyrrhotite superstructures (4C - Fe7S8/5C - Fe9S10) in Ni-Cu sulphide mineral processing. *Can. J. Chem. Eng.* 96 (5), 1185–1206. doi:10.1002/cjce.23099

Nahanni National Park Reserve (2010). Naha dehe - Nahanni national Park Reserve of Canada. Available at: https://www.pc.gc.ca/en/pn-np/nt/nahanni/visit/~/media/EC085A2C67574FFF912A6AFBE39D3488.ashx (Accessed December 10, 2023).

Natural Resources Canada (2001). Canada. Available at: https://ftp.maps.canada.ca/pub/nrcan_rncan/raster/atlas_6_ed/reference/bilingual/canada01.pdf (Accessed December 10, 2023).

Natural Resources Canada (2022). *The Canadian critical minerals strategy*.

Nicholson, R. V., Tibble, P. A., and Williams, G. (1997). A Survey of *in situ* oxygen consumption rates on sulphide tailings: investigations on exposed and covered tailings. *MEND*.

Nikonow, W., Rammlmair, D., and Furche, M. (2019). A multidisciplinary approach considering geochemical reorganization and internal structure of tailings impoundments for metal exploration. *Appl. Geochem.* 104, 51–59. doi:10.1016/j.apgeochem.2019.03.014

North American Tungsten Corporation LTD (2020). *Engagement plan V2*.

Paktunc, A. D. (1999). Mineralogical constraints on the determination of neutralization potential and prediction of acid mine drainage. *Environ. Geol.* 39 (2), 103–112. doi:10.1007/s002540050440

Prescher, C., and Prakapenka, V. B. (2015). DIOPTAS: a program for reduction of two-dimensional X-ray diffraction data and data exploration. *High Press. Res.* 35 (3), 223–230. doi:10.1080/08957959.2015.1059835

Rasmussen, K. L., Lentz, D. R., Falck, H., and Pattison, D. R. M. (2011). Felsic magmatic phases and the role of late-stage aplitic dykes in the formation of the world-

class Cantung Tungsten skarn deposit, Northwest Territories, Canada. *Ore Geol. Rev.* 41 (1), 75–111. doi:10.1016/j.oregeorev.2011.06.011

Sarker, S. K., Haque, N., Bhuiyan, M., Bruckard, W., and Pramanik, B. K. (2022). Recovery of strategically important critical minerals from mine tailings. *J. Environ. Chem. Eng.* 10 (3), 107622. doi:10.1016/j.jece.2022.107622

SRK Consulting Inc (2023). *Cantung mine tailings storage facilities 2022 dam safety review*. Vancouver, BC: FINAL REPORT.

Tang, X., and Chen, Y. (2022). A review of flotation and selective separation of pyrrhotite: a perspective from crystal structures. *Int. J. Min. Sci. Technol.* 32 (4), 847–863. doi:10.1016/j.ijmst.2022.06.001

Tetra Tech (2022). *Annual geotehcnical inspection - tailings containment area, Cantung mine, tungsten, NT*.

Ulrich, B. (2019). "Practical thoughts regarding filtered tailings," in *Paste 2019*. Editors A. J. C. Paterson, A. B. Fourie, and D. Reid (Cape Town, South Africa: Australian Centre for Geomechanics).

URS (2000). "URS Norecol Dames and Moore, SRK consulting Inc, SENES consultants ltd, and BC research Inc," in *MEND manual volume 3 - prediction*. Editors Manual, MEND, Tremblay, G. A., and Hogan, C. M. 5.4.2c ed (New York: INC).

U.S. Geological Survey (2022). 2022 final list of critical minerals. *U.S. Geol. Surv. Dep. Interior*.

Zinck, J., Tisch, B., Cheng, T., and Cameron, R. (2019). "Mining value from waste initiative: towards a low carbon and circular economy," in *Rewas 2019* (Germany: Springer International Publishing).